Relative Ligand-Binding Free Energies Calculated from Multiple Short QM/MM MD Simulations

Ryde, Ulf; Olsson, Martin; Steinmann, Casper

Published in:
Journal of Chemical Theory and Computation

DOI:
10.1021/acs.jctc.8b00081

2018

Document Version:
Peer reviewed version (aka post-print)

Relative Ligand-Binding Free Energies Calculated from Multiple Short QM/MM MD Simulations

Casper Steinmann,*,†,‡ Martin A. Olsson,‡ and Ulf Ryde*,‡

†*Department of Chemistry and Bioscience, Aalborg University, Frederik Bajers Vej 7H, DK-9220 Aalborg, Denmark*

‡*Department of Theoretical Chemistry, Lund University, Chemical Centre, P. O. Box 124, SE-221 00 Lund, Sweden*

E-mail: css@bio.aau.dk; ulf.ryde@teokem.lu.se

Abstract

We have devised a new efficient approach to compute combined quantum mechanical (QM) and molecular mechanical (MM, i.e. QM/MM) ligand-binding relative free energies. Our method employs the reference-potential approach with free-energy perturbation both at the MM level (between the two ligands) and from MM to QM/MM (for each ligand). To ensure that converged results are obtained for the MM→QM/MM perturbations, explicit QM/MM molecular dynamics (MD) simulations are performed with two intermediate mixed states. To speed up the calculations, we utilize the fact that the phase space can be extensively sampled at the MM level. Therefore, we run many short QM/MM MD simulations started from snapshots of the MM simulations, instead of a single long simulation. As a test case, we study the binding of nine cyclic carboxylate ligands to the octa-acid deep cavitand. Only the ligand is in the QM system, treated with the semi-empirical PM6-DH+ method. We show that for eight of the ligands, we obtain well converged results with short MD simulations (1–15 ps). However, in one case, the convergence is slower (∼50 ps) owing to a mismatch between the

conformational preferences of the MM and QM/MM potentials. We test the effect of initial minimization, the need of equilibration and how many independent simulations are needed to reach a certain precision. The results show that the present approach is about four times faster than using standard MM→QM/MM free-energy perturbations with the same accuracy and precision.

1 Introduction

Predicting the binding of a small molecule (L for ligand) to a biological macromolecule (R for receptor), i.e. the free energy of the reaction R + L → RL, remains one of the greatest challenges of computational chemistry. Accurate predictions of such binding free energies could have a large impact on areas such as rational drug design, for which the need to perform expensive experiments would be reduced.

According to statistical mechanics, the free-energy difference can be expressed as averages over molecular configurations of the atomic coordinates, which can be obtained from molecular dynamics (MD) or Monte Carlo simulations. In principle, proper free energies can be obtained from free-energy perturbation (FEP) calculations with the energies estimated by exponential averaging (EA, Zwanzig equation),[1] thermodynamic integration,[2] Bennett acceptance ratio (BAR)[3,4] or similar methods. The difference in binding free energies of two similar ligands (L_0 and L_1) can be obtained by calculating the energy difference between the two ligands when bound to the receptor macromolecule and when free in solution.[5] However, such calculations converge only when the energy difference is small, i.e. when there is enough overlap in the energy functions of the two ligands so that they sample the same part of the phase space. In practice, this is seldom the case and this problem is solved by dividing the transformation between the two ligands into several small steps, employing an interpolated potential, using a coupling parameter λ ($0 \leq \lambda \leq 1$):

$$E(\lambda) = (1 - \lambda)E_0 + \lambda E_1, \tag{1}$$

where E_0 and E_1 are the potentials for L_0 and L_1, respectively. Moreover, FEP is guaranteed to yield correct results only if the energy function is perfect and the sampling is exhaustive. The latter point has historically implied the use of molecular mechanics (MM) force fields for the sampling, because such calculations are cheap enough to allow for long simulation times that provide a representative ensemble of configurations.[6,7]

However, the MM force field is far from a perfect energy function and therefore, there has been quite some interest to use quantum mechanical (QM) methods in the FEP simulations.[8] For the binding of a ligand to a bio-macromolecule receptor, this would require the use of combined QM/MM methods.[9,10] Such calculations can be performed at many levels of approximations, as is illustrated in Scheme 1. The arrow at the top of the figure, represents

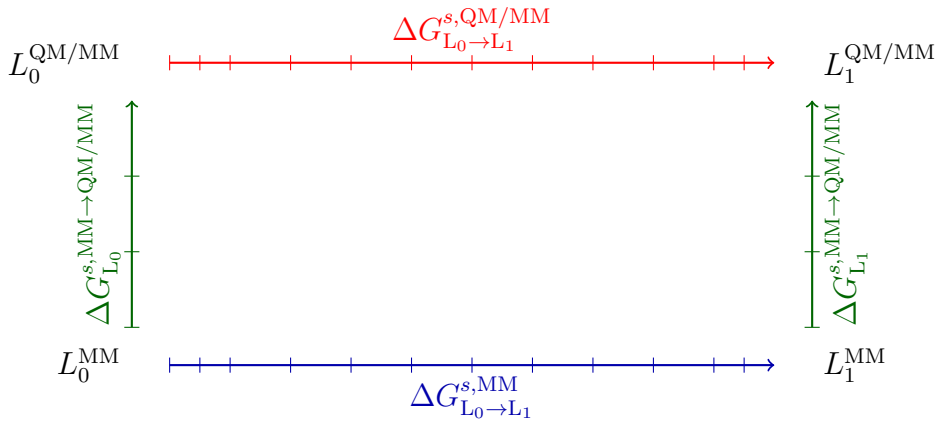

Scheme 1: Thermodynamic cycle employed to estimate the relative binding free energy between two ligands (L_0 and L_1) at the QM/MM level of theory, $\Delta G^{s,\mathrm{QM/MM}}_{\mathrm{L_0\to L_1}}$, for state s (i.e. either for the ligand free in solution or when bound to the host). In the reference-potential methods, $\Delta G^{s,\mathrm{QM/MM}}_{\mathrm{L_0\to L_1}}$ is estimated from the change in free energy at the MM level of theory, $\Delta G^{s,\mathrm{MM}}_{\mathrm{L_0\to L_1}}$ (lower horizontal arrow). The free energies are corrected at the end points with a FEP in methods space, from MM to QM/MM, $\Delta G^{s,\mathrm{MM\to QM/MM}}_{\mathrm{L_i}}$. The bars on the arrows illustrate that each perturbation is divided into several intermediate states, characterized by the λ coupling parameter for the horizontal perturbations and by the Λ parameter for the vertical perturbations.

a full FEP calculation at the QM/MM level, $\Delta G^{s,\mathrm{QM/MM}}_{\mathrm{L_0\to L_1}}$, where s, represents either the ligand bound to the receptor or free in solution. The net binding free energy, $\Delta\Delta G^{\mathrm{bind}}_{\mathrm{L_0\to L_1}}$, is

the difference of those two terms:

$$\Delta\Delta G^{\mathrm{bind,QM/MM}}_{\mathrm{L_0\to L_1}} = \Delta G^{\mathrm{bound,QM/MM}}_{\mathrm{L_0\to L_1}} - \Delta G^{\mathrm{free,QM/MM}}_{\mathrm{L_0\to L_1}}. \quad (2)$$

Such FEP calculations have been employed a few times for protein binding energies,[11–14] using a semi-empirical QM method and treating only the ligand by QM. The reason for this is that long MD simulations and many intermediate states are required to get converged and reliable results (for example we run $2 \times 18 \times 1.5$ ns $= 54$ ns simulations for each ligand pair in our recent study[14]). This has spurred the development of computationally cheaper alternatives, in particular reference-potential methods[15–20] developed independently by Warshel[15] and Gao[16,17] more than 25 years ago. These take advantage of the corresponding FEP calculations at the MM level ($\Delta G^{s,\mathrm{MM}}_{\mathrm{L_0\to L_1}}$ at the bottom of Scheme 1), which are much cheaper. By using the thermodynamic cycle in Scheme 1, the $\Delta G^{s,\mathrm{QM/MM}}_{\mathrm{L_0\to L_1}}$ free energy can be obtained from $\Delta G^{s,\mathrm{MM}}_{\mathrm{L_0\to L_1}}$ by performing FEP simulations in method space to convert the MM potential to a QM/MM (or QM) potential ($\Delta G^{s,\mathrm{MM\to QM/MM}}_{\mathrm{L_i}}$ for the two ligands L_0 and L_1 shown as vertical arrows in Scheme 1), i.e.

$$\Delta\Delta G^{\mathrm{bind,QM/MM}}_{\mathrm{L_0\to L_1}} = \Delta\Delta G^{\mathrm{bind,MM}}_{\mathrm{L_0\to L_1}} - \Delta\Delta G^{\mathrm{bind,MM\to QM/MM}}_{\mathrm{L_0}} + \Delta\Delta G^{\mathrm{bind,MM\to QM/MM}}_{\mathrm{L_1}}. \quad (3)$$

Again, several approaches can be used to calculate $\Delta G^{s,\mathrm{MM\to QM/MM}}_{\mathrm{L_i}}$. The most common approach is to try to estimate it by exponential averaging. If this converges in a single step (ssEA), no MD simulations at the QM/MM level of theory are needed because the energies can be calculated directly by single-point QM calculations on snapshots already available from the FEP calculation of $\Delta G^{s,\mathrm{MM}}_{L_0\to L_1}$.[15,18,21] Alternatively, $\Delta G^{s,\mathrm{MM\to QM/MM}}_{\mathrm{L_i}}$ can be calculated by the non-Boltzmann BAR approach (NBB), which employs the fact that BAR normally gives better results than EA, especially when the overlap of the energy functions is poor.[22] However, NBB requires QM calculations on an additional intermediate state and therefore is twice as expensive as ssEA.[21] Moreover, theoretical considerations have indicated

that ssEA performs slightly better than NBB both in theory and in practice.[23]

NBB and ssEA have been used in recent studies of binding free energies.[23–27] However, several of these (especially when including more than the ligand in the QM system[25,26]) showed serious problems to converge the free energies, simply because the MM and QM/MM potentials are too dissimilar to allow $\Delta G^{s,\mathrm{MM}\rightarrow\mathrm{QM/MM}}_{\mathrm{L_i}}$ to be calculated based solely on snapshots from MD simulations at the MM level. For enzyme reaction energies, the problem is often solved by keeping the QM system fixed in the FEP calculations,[15,18,19] but that does not seem to be a useful approach for ligand binding, for which entropy effects of the ligand are important. With a semi-empirical QM method, we have managed to obtain $\Delta G^{s,\mathrm{MM}\rightarrow\mathrm{QM/MM}}_{\mathrm{L_i}}$ energies that were seemingly converged to within 1 kJ mol^{-1} employing 720 000 QM calculations per ligand, but only when using ssEA with the cumulant approximation to the second order[28,29] (ssEAc; i.e. assuming that the energy distribution is Gaussian).[21] Plain ssEA and NBB gave results with an estimated uncertainty of 2–7 kJ mol^{-1}.

This number of QM/MM energy calculations corresponds to up to 1.4 ns of MD simulations. Therefore, we tested in our most recent study to actually run QM/MM MD simulations.[14] We performed both full QM/MM FEP calculations (upper arrow in Scheme 1) and reference-potential calculations, but dividing the calculations of $\Delta G^{s,\mathrm{MM}\rightarrow\mathrm{QM/MM}}_{\mathrm{L_i}}$ (vertical arrows in Scheme 1) into several steps denoted by the coupling parameter Λ for the hybrid energy function

$$E(\Lambda) = (1-\Lambda)E_{\mathrm{MM}} + \Lambda E_{\mathrm{QM/MM}}, \tag{4}$$

connecting the MM energy (E_{MM}) and the QM/MM energy ($E_{\mathrm{QM/MM}}$; again $0 \leq \Lambda \leq 1$; we use Λ to avoid confusion with the λ parameter for the horizontal perturbations in Scheme 1). Thus, the calculation of $\Delta G^{s,\mathrm{MM}\rightarrow\mathrm{QM/MM}}_{\mathrm{L_i}}$ employed expensive QM/MM MD simulations. We showed that the two approaches gave identical results, within the statistical uncertainty. For the direct calculation of $\Delta G^{s,\mathrm{QM/MM}}_{\mathrm{L_0}\rightarrow\mathrm{L_1}}$, our overlap measures indicated that a total of 18 λ values were needed (but this number may of course depend on both the system studied and the potential used). For $\Delta G^{s,\mathrm{MM}\rightarrow\mathrm{QM/MM}}_{\mathrm{L_i}}$, it was enough to consider four Λ values.

Consequently, the latter approach was more effective. However, since each state required 1.5 ns MD simulations, this approach was much more demanding than the ssEAc calculations. On the other hand, ssEAc depends on the accuracy of the cumulant approximation and it is normally performed only for interaction energies (to improve convergence) and not for the more correct total energies. Moreover, there were indications that the results were still not fully converged with independent calculations of the same energy component yielding results that varied by up to 9 kJ/mol.[21] Therefore, the reference-potential calculations with explicit QM/MM MD simulations seemed to be more reliable. Other studies have also showed that converged binding affinities can be obtained with sampling at the QM/MM level.[27,30,31] A similar approach (paradynamics) has been used for enzyme reactions, but normally with only two Λ states[15,32,33]), but for our binding affinities, this gave poor overlap and not converged results.[14] Another study has recently reached similar conclusions.[34]

In this paper, we use a similar method, i.e. the reference-potential approach, calculating $\Delta G_{\mathrm{L_i}}^{s,\mathrm{MM}\rightarrow\mathrm{QM/MM}}$ with four Λ states, but investigate whether the simulations can be sped up, exploiting the fact that we can thoroughly explore the phase space for each ligand with MD simulations at the MM level. Therefore, we make the QM/MM MD simulations very short and instead run many of them. We investigate if we still can reproduce the previous results and examine how long the simulations need to be, how much equilibrium time is needed and how many independent calculations are needed to reach a certain precision. The results show that significant time can be saved by such an approach without compromising the accuracy for most systems.

2 Computational Details

2.1 Ligands and MM calculations

We have studied the MM→QM/MM contribution to the binding free energies for nine cyclic carboxylate ligands bound to the octa-acid (OA) deep-cavity cavitand from the SAMPL4[35,36]

competition, shown in Scheme 2. The aim is to improve the estimates of the relative binding free energies in the following eight ligand transformations: MeBz→Bz, EtBz→MeBz, pClBz→Bz, mClBz→Bz, Hx→Bz, MeHx→Hx, Hx→Pen and Hx→Hep (the names of the ligands are defined in Scheme 2). The underlying MM simulations and estimates of the

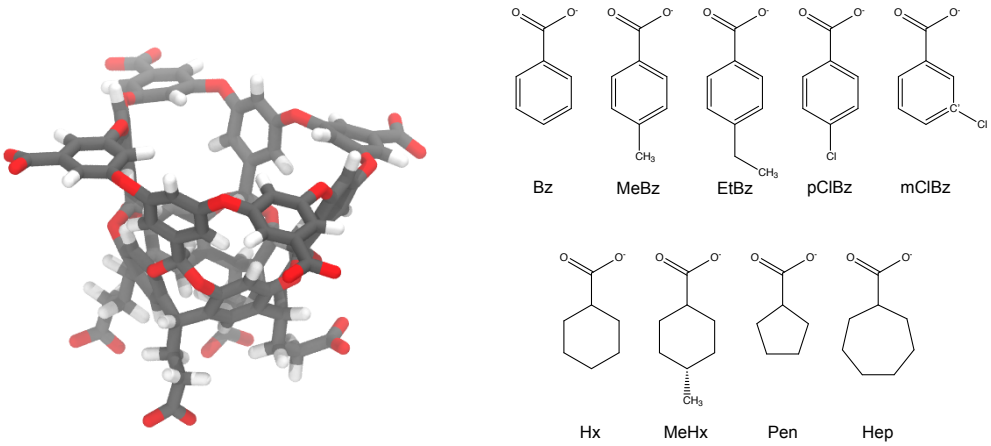

Scheme 2: Octa-acid host (left) and ligands considered in this study (right).

relative binding free energy at the MM level of theory were taken from our previous work on the same system.[21,25] In those, the general Amber force field[37] (GAFF) was used for both the host and the ligands, with partial atomic charges derived from restrained electrostatic potential fits[38] (RESP), obtained at the HF/6-31G* level of theory.

2.2 QM/MM Free-Energy Simulations

For each ligand, either bound to the host or free in water solution, we extracted 100 snapshots from the previous MD simulations at the MM level. For each of these snapshots, we ran a 50 ps QM/MM FEP calculation using four Λ values ($\Lambda = 0.0, 0.333, 0.666, 1.0$). In our previous study, we studied thoroughly the convergence of the free energies with respect to the number of Λ values and showed that four Λ values is needed.[14] We checked that this still applies also for the present calculations by performing one of the simulations also with nine Λ values. The results in Figure S1 in the supporting information show that the two simulations give identical results within statistical uncertainty. The QM/MM MD simulations were done

with the *sander* module of the Amber 14[39,40] software using the dual-topology scheme. Only the ligand was included in the QM region, whereas the host and all solvent molecules were in the MM system. The free ligands were solvated with roughly 3000 explicit water molecules and the host–ligand complex was solvated by about 5500 water molecules. The QM calculations were performed at the semi-empirical PM6-DH+[41] level of theory. PM6-DH+ was selected because it was employed in our previous study of the same system[14] (so that we can use those results as a calibration) and it is one of the most accurate semi-empirical methods available in the Amber software, employing dispersion and hydrogen-bond corrections that are parametrized to yield reliable non-covalent interactions. In all calculations, the temperature was kept at 300 K using Langevin dynamics with a collision frequency of 2 ps^{-1}.[42] The pressure was kept at 1 atm using Berendsen's weak-coupling isotropic algorithm with a relaxation time of 1 ps.[43] Long-range electrostatics were handled by particle-mesh Ewald summation,[44] whereas Lennard-Jones interactions were truncated beyond 8 Å. All QM/MM MD simulations were run without any restraints and with a time step of 1 fs.

For each snapshot, free-energy differences were calculated over the four Λ-windows with the multistate Bennett acceptance ratio (MBAR) approach, as implemented in the pyMBAR software.[45] All free-energy estimates are based on total energies, in contrast to many simplified approaches that employ QM/MM interaction energies.[8,21,23,25]

3 Results and Discussion

In this paper, we studied whether calculations of

$$\Delta\Delta G_{\mathrm{L_i}}^{\mathrm{MM}\rightarrow\mathrm{QM/MM}} = \Delta G_{\mathrm{L_0}\rightarrow\mathrm{L_1}}^{\mathrm{bound,QM/MM}} - \Delta G_{\mathrm{L_0}\rightarrow\mathrm{L_1}}^{\mathrm{free,QM/MM}} \tag{5}$$

with the reference-potential approach can be sped up by using many short QM/MM simulations, exploiting the fact that the cheap MM simulations already have extensively explored

the phase space. To this aim, we have studied the binding of nine small cyclic carboxylate molecules (shown in Scheme 2) to the octa-acid deep-cavity host. We have already studied this system in several previous studies, giving us proper reference results.[14,21,25] In those papers, we also compared the compuational and experimental results, whereas in this paper, we concentrate on the convergence of the MM→QM/MM perturbation and how the simulations can be sped up. We also compared the results of the reference-potential approach with direct QM/MM FEP calculations (i.e. following the red arrow in Scheme 1), showing that the two approches give identical results within the statistical uncertainty.[14] In separate subsections, we will describe first the convergence of $\Delta\Delta G_{\mathrm{L_i}}^{\mathrm{MM\rightarrow QM/MM}}$ with respect to the simulation time, then the number of independent simulations needed and finally, whether the results can be improved by omitting an initial part of the simulation as an equilibration period.

3.1 Convergence of $\Delta\Delta G_{\mathrm{L_i}}^{\mathrm{MM\rightarrow QM/MM}}$

In this section, we discuss how the MM→QM/MM free-energy change for a ligand $\mathrm{L_i}$, $\Delta\Delta G_{\mathrm{L_i}}^{\mathrm{MM\rightarrow QM/MM}}$, converges as a function of simulation length for the nine ligands in this study. The free-energy changes were calculated using MBAR at simulation lengths (τ) ranging from 1 to 50 ps. We computed the mean of $\Delta\Delta G_{\mathrm{L_i}}^{\mathrm{MM\rightarrow QM/MM}}$ and standard error of the mean ($\mathrm{SE_{L_i}} = s/\sqrt{N}$ where s is standard deviation) over the N trajectories included in the averaging procedure ($N = 100$ if not otherwise stated). These results are presented in Figure 1, in which we also show the $\Delta\Delta G_{\mathrm{L_i}}^{\mathrm{MM\rightarrow QM/MM}}$ values obtained from our previous study with full QM/MM FEP simulations (Table 1 in Ref 14; 1.5 ns MD simulations for four Λ values) as black dashed lines with uncertainties plotted as gray shaded areas. These results are used as reference values for the new (shorter) simulations. We have included markers (dashed gray horizontal lines) at ± 1 kJ mol^{-1} from the reference value to indicate a satisfactory accuracy, in line with previous efforts to quantify convergence.[14,21] It also represents an approximate confidence interval for the difference between the old results

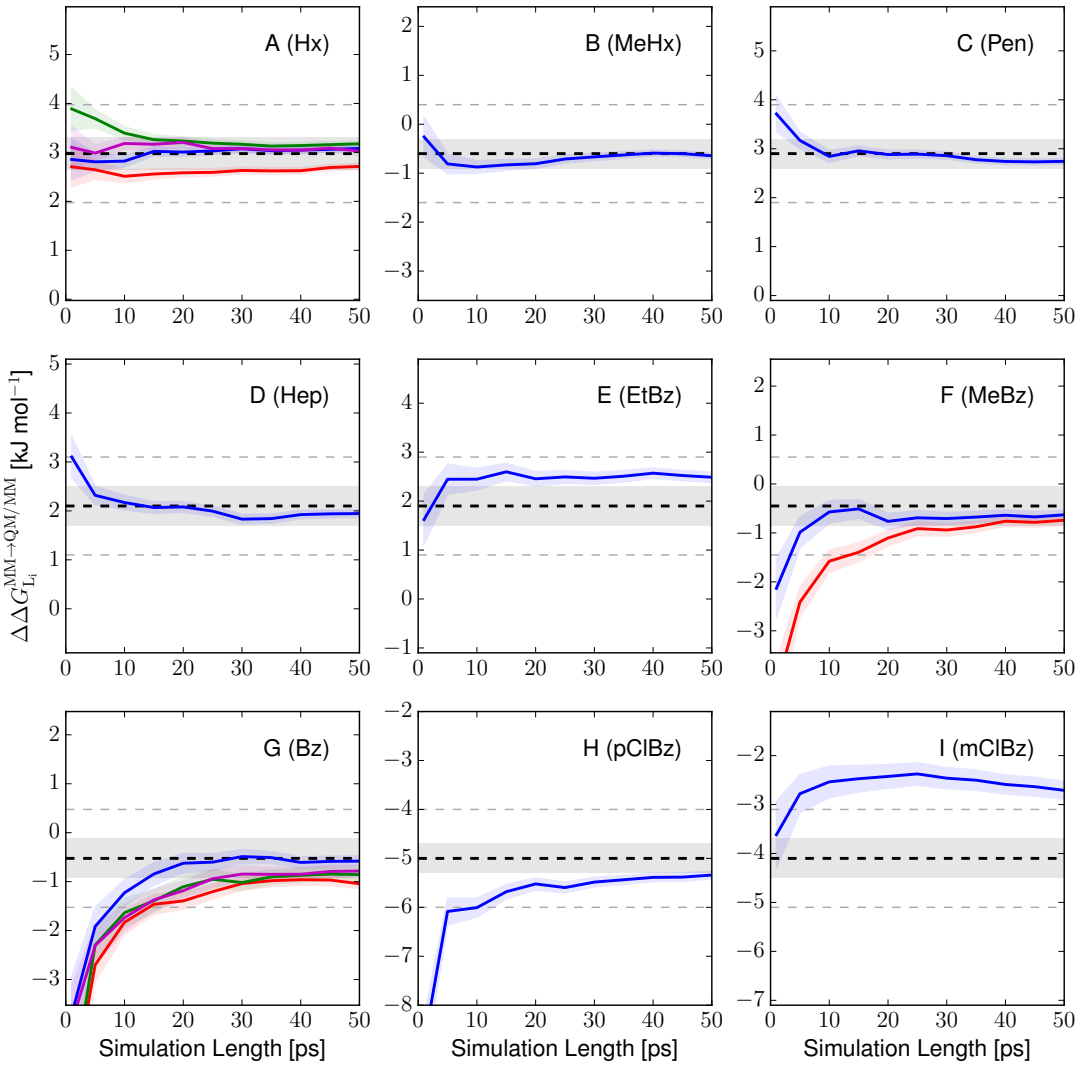

Figure 1: Convergence profiles of $\Delta\Delta G_{L_i}^{MM\rightarrow QM/MM}$ (eq 5) for the nine ligands in this study as a function of the simulation time per Λ-window. For ligands, Bz, MeBz and Hx two or four independent simulations were run, shown with separate curves in different colors.

(standard errors of 0.3–0.4 kJ mol^{-1}) and new results (standard errors decreasing from 0.4 to 0.1 kJ mol^{-1} when the simulation time is increased, employing a t-factor of 1.96 (95% confidence). We emphasize that the time shown on the x-axis in Figure 1 is given in picoseconds and represents the simulation time for each Λ window. This serves to elucidate how

fast $\Delta\Delta G_{\mathrm{L_i}}^{\mathrm{MM}\rightarrow\mathrm{QM/MM}}$ converges with the length of the simulations. QM/MM minimizations prior to QM/MM MD simulations had negligible effects on the convergence (see Figure S2 in the Supporting Information) and was therefore not further investigated.

The results show that for five of the ligands (Hx, MeHx, Pen, Hep and EtBz shown in panels A to E in Figure 1), $\Delta\Delta G_{\mathrm{L_i}}^{\mathrm{MM}\rightarrow\mathrm{QM/MM}}$ is converged to within 1 kJ mol^{-1} of the reference value already from the first picosecond of the simulation. For $\Delta\Delta G_{\mathrm{Hx}}^{\mathrm{MM}\rightarrow\mathrm{QM/MM}}$, we have results from four independent sets of simulations (taken from the transformations Hx→Bz, MeHx→Hx, Hx→Pen and Hep→Hx) and these are shown in different colors in Figure 1A. It is satisfying that the four simulations give results that agree with each other within 1 kJ mol^{-1} already from 1 ps simulation time. This is better than in our previous work,[14] in which the variation was 1.5 kJ mol^{-1} (2.1–3.6 kJ mol^{-1}) for four Λ values and a total of nine Λ values were needed to bring the variation down to 0.3 kJ mol^{-1}. For four of the ligands, Hx, MeHx, Pen, Hep, the new results agree with the reference values within 0.3 kJ mol^{-1} at the end of the simulation (50 ps), and actually already after 1–20 ps simulation time. However, for EtBz, there is a 0.6 kJ mol^{-1} difference between the new results (apparently converged already after 5 ps) and the reference value (Figure 1E). In principle, this is no problem, as the new result still falls within the 95% (and also 90%) confidence interval of the reference results (the gray area in the figure marks a single standard deviation). Yet, considering the good accuracy and precision of the other new calculations and the clear convergence of the results, it seems likely that the new result is more accurate. This is confirmed by the fact that in the previous investigation, nine Λ values gave a slightly larger $\Delta\Delta G_{\mathrm{EtBz}}^{\mathrm{MM}\rightarrow\mathrm{QM/MM}}$, 2.1±0.5 kJ mol^{-1},[14] closer to the new result.

For three of the ligands, MeBz, Bz and pClBz, it is slightly more difficult to converge $\Delta\Delta G_{\mathrm{L_i}}^{\mathrm{MM}\rightarrow\mathrm{QM/MM}}$ to within 1 kJ mol^{-1} of the reference values. For $\Delta\Delta G_{\mathrm{MeBz}}^{\mathrm{MM}\rightarrow\mathrm{QM/MM}}$, shown in Figure 1F, convergence is achieved after 3 and 10 ps for the two independent calculations (based on results for the MeBz→Bz and EtBz→MeBz transformations) and the final results (at 50 ps) agree closely with each other and with the reference value. The free

energy change for the Bz ligand, $\Delta\Delta G_{\mathrm{Bz}}^{\mathrm{MM}\rightarrow\mathrm{QM/MM}}$, shown in Figure 1G, has slightly longer convergence times ranging from 9 to 15 ps for the four independent sets of simulations (taken from the transformations MeBz→Bz, pClBz→Bz, mClBz→Bz and Hx→Bz). The pClBz ligand shows similar convergence, in that it requires roughly 10 ps of simulation time to converge $\Delta\Delta G_{\mathrm{pClBz}}^{\mathrm{MM}\rightarrow\mathrm{QM/MM}}$, despite deviating by more than 3 kJ mol^{-1} initially, as shown in Figure 1H.

However, the results for the mClBz ligand is much different from those of the other eight ligands: Even after 50 ps, $\Delta\Delta G_{\mathrm{mClBz}}^{\mathrm{MM}\rightarrow\mathrm{QM/MM}}$ deviates by 1.4 kJ mol^{-1} from the reference value and the results do not seem to be converged. $\Delta\Delta G_{\mathrm{mClBz}}^{\mathrm{MM}\rightarrow\mathrm{QM/MM}}$ attains a maximum (–2.2 kJ mol^{-1}) at 25 ps and then slowly decreases during the remainder of the simulation time. Therefore, we extended the simulation time to 150 ps and the results are shown in

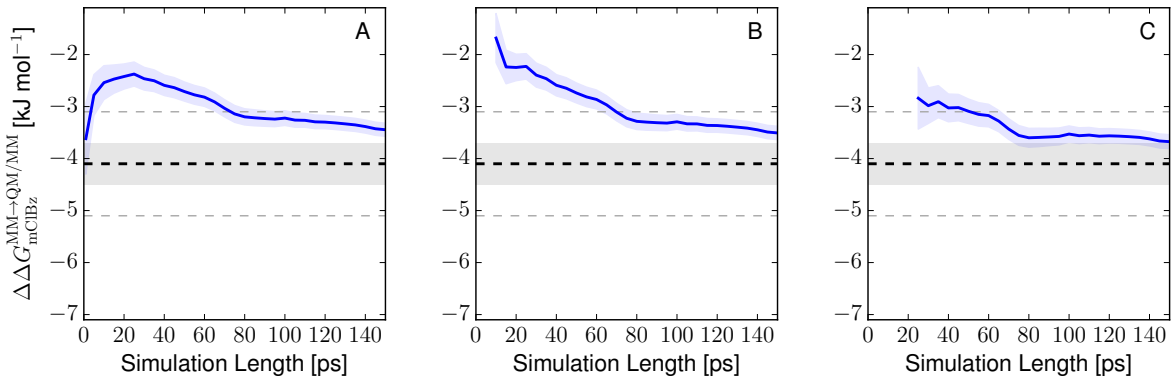

Figure 2: Results of extended (150 ps) simulations for the mClBz ligand. In A), all data were employed, whereas in B) and C) the first 10 ps and 25 ps were omitted in the estimate of $\Delta\Delta G_{\mathrm{mClBz}}^{\mathrm{MM}\rightarrow\mathrm{QM/MM}}$.

Figure 2A, in which it can be seen that the results agrees within 1 kJ mol^{-1} of the reference value after 75 ps, but the curve is still decreasing at the end of the simulation. The results do not change much if the first 10 ps of the simulation is discarded as an equilibration period, besides that the maximum is increased and moves to 10 ps (Figure 2B). However, if the equilibration period is extended to 25 ps (Figure 2C), convergence to within 1 kJ mol^{-1} is reached already after 50 ps simulation time and $\Delta\Delta G_{\mathrm{mClBz}}^{\mathrm{MM}\rightarrow\mathrm{QM/MM}}$ converges to a nearly

constant value after 80 ps time. This indicates that mClBz undergoes a slow conformational change, giving less negative $\Delta\Delta G^{\mathrm{MM}\rightarrow\mathrm{QM/MM}}_{\mathrm{mClBz}}$ at the beginning of the simulation, which takes a very long time to average away.

A thorough investigation of the energies and the simulations (described in the Supporting Information) showed that the slow convergence can be traced to the simulation of the complex and in particular the position of the Cl atom in the host. To illustrate this difference, we defined the vector between the centroid of the upper and lower ring in the octa-acid host, $\mathbf{R}_{\mathrm{OA}}$, shown in Figure S13. Then, the angle between $\mathbf{R}_{\mathrm{OA}}$ and the C'–Cl vector (see Scheme 2) in mClBz was followed during the MD simulations. From the histograms in Figure 3, it can be seen that at 10 ps simulation time, there is only a minor difference in the angles attained with the MM and QM/MM potentials, both showing a small peak around ∼30° (Cl atom points almost downwards in the host) and a larger and broader peak at ∼60° (Cl atom points towards the side of the host). However, as the simulation time is increased, a shift in

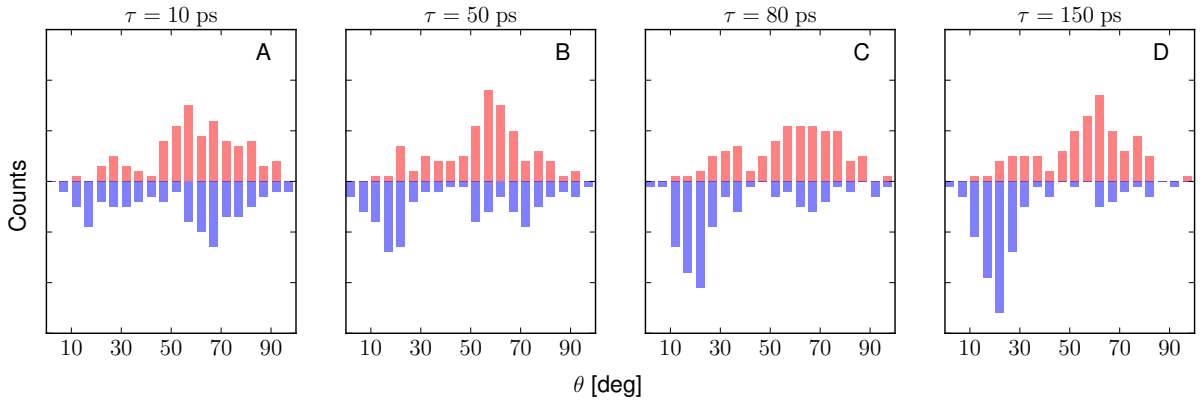

Figure 3: Histograms of the angle between the host $\mathbf{R}_{\mathrm{OA}}$ and mClBz ligand C'–Cl vectors at different simulation times. The upper (red) histograms are for the MM potential at $\Lambda = 0.0$ and the blue histograms are for the QM/MM potential at $\Lambda = 1.0$.

the angles obtained with the QM/MM potential is observed towards $< 30°$ (Figure 3B–D), whereas the angles for the MM potential do not appear to change significantly. From the results presented in Figure 3, it is clear that this conformational change takes a long time (∼50 ps) and it is the reason for the slow convergence observed in Figures 1 and 2. The problem probably stems from sub-optimal parameters of the chlorine atom in the GAFF

force field of mClBz and may be ameliorated by a re-parametrization of the van der Waals parameters.

In summary we find that the MM→QM/MM calculations using our approach works well for eight of nine ligands, with convergence of $\Delta\Delta G_{\mathrm{L_i}}^{\mathrm{MM\rightarrow QM/MM}}$ within 1–15 ps, considerably reducing the cost of the simulations. However, for a single system, a significant difference between the conformations attained by the ligand in the MM and QM/MM potential is observed and a proper equilibration of this difference takes ∼50 ps.

3.2 Effect of Equilibration Period

For the mClBz ligand, it was seen in Figure 2 that the results were improved if the initial 25 ps simulations were discarded as an equilibrium period. It is possible that also the other results could be improved by such a procedure. Therefore, we have tested to discard the first 1 or 5 ps of the simulations. The results are shown in Figures S14 and S15 in the Supporting Information. It is seen that for MeBz, Bz and pClBz, the results strongly improve if some data from the first part of the simulation is discarded. If 1 ps is discarded, the pClBz simulation is converged already from start, whereas $\Delta\Delta G_{\mathrm{MeBz}}^{\mathrm{MM\rightarrow QM/MM}}$ converges within 3–7 ps (4–13 ps without any equilibration) and $\Delta\Delta G_{\mathrm{Bz}}^{\mathrm{MM\rightarrow QM/MM}}$ converges within 4–7 ps, which is an even larger improvement (8–14 ps without any equilibration). With 5 ps equilibration, all seven free energies are converged already at the start of the sampling period (5 ps). For none of the ligands, the final result (at 50 ps) changes if data is discarded as equilibration.

The following systematic approach can be used to determine how much time (t_{eq}) at the start of the simulation should be discarded as equilibration. We define as our reference $\Delta\Delta G_{\mathrm{L_i}}^{\mathrm{MM\rightarrow QM/MM}}$ (with standard error $\mathrm{SE}_{\mathrm{L_i}}$) computed as the result obtained by integrating from t_{eq} to the end of the simulation ($t_{\mathrm{sim}} = 50$ ps) using the following notation $\Delta\Delta G_{\mathrm{L_i}}(t_{\mathrm{eq}}, t_{\mathrm{sim}})$ for the free energy and $\mathrm{SE}_{\mathrm{L_i}}(t_{\mathrm{eq}}, t_{\mathrm{sim}})$ for the standard error (omitting the superscript MM→QM/MM for simplicity). We then test if the first picosecond of the simulation can be discarded based on whether it deviates significantly from the reference results

by a simple t-test: We compute $\Delta\Delta G_{\mathrm{L_i}}(t_{\mathrm{eq}}, t_{\mathrm{eq}} + 1\ \mathrm{ps})$ and $\mathrm{SE}_{\mathrm{L_i}}(t_{\mathrm{eq}}, t_{\mathrm{eq}} + 1\ \mathrm{ps})$ and measure whether these two free energy distributions overlap by comparing the absolute difference in free energies and the composite error of the two standard errors with 95 % confidence following Nicholls:[46]

$$|\Delta\Delta G_{\mathrm{L_i}}(t_{\mathrm{eq}}, t_{\mathrm{sim}}) - \Delta\Delta G_{\mathrm{L_i}}(t_{\mathrm{eq}}, t_{\mathrm{eq}} + 1\ \mathrm{ps})| < t_{95\%} \cdot \mathrm{CE}_{\mathrm{L_i}}. \tag{6}$$

where the composite error for ligand $\mathrm{L_i}$, $\mathrm{CE}_{\mathrm{L_i}}$, is

$$\mathrm{CE}_{\mathrm{L_i}} = \sqrt{\left(\mathrm{SE}_{\mathrm{L_i}}(t_{\mathrm{eq}}, t_{\mathrm{sim}})\right)^2 + \left(\mathrm{SE}_{\mathrm{L_i}}(t_{\mathrm{eq}}, t_{\mathrm{eq}} + 1\ \mathrm{ps})\right)^2}$$

If the inequality in eq 6 does not hold, the first picosecond is discarded as equilibration time so $t_{\mathrm{eq}} = t_{\mathrm{eq}} + 1$ ps and both $\Delta\Delta G_{\mathrm{L_i}}(t_{\mathrm{eq}}, t_{\mathrm{sim}})$ and $\Delta\Delta G_{\mathrm{L_i}}(t_{\mathrm{eq}}, t_{\mathrm{eq}} + 1\ \mathrm{ps})$ are recomputed and eq 6 is re-evaluated until it holds. This procedure was applied to all ligands (except the diverging mClBz ligand) for $\Delta\Delta G_{\mathrm{L_i}}^{\mathrm{MM}\rightarrow\mathrm{QM/MM}}$, but also on the individual $\Delta G_{\mathrm{L_i}}^{s,\mathrm{MM}\rightarrow\mathrm{QM/MM}}$ values for the ligand free in solution or bound to the host. These results are presented in Table 1.

It can be seen that the equilibration time in general is shorter for $\Delta\Delta G$ than for ΔG^s. This is in agreement with the data presented in Table S1 and Figures S3–S11, discussed in Section 3 of the SI. The reason is simply that the ΔG^s terms are appreciably larger in magnitude (500–800 kJ mol^{-1}) than $\Delta\Delta G$. For $\Delta\Delta G$, t_{eq} is 1–3 ps for the aromatic ligands (5 ps for MeBz) and 0 ps for the non-aromatic ligands (1 ps for Hep). For ligands free in solution, the equilibration times are 2–6 ps and when bound to the octa-acid host they are 2–4 ps, except for one case each for MeBz (8 ps) and Hx (10 ps). Apart from the latter two outliers, the ligands bound to the octa-acid host equilibrate faster than when they are free in solution.

Table 1: Equilibration period, t_{eq} (in ps), for the various ligands, employing the results after 50 ps as the reference value. t_{eq} was calculated for either $\Delta\Delta G_{\mathrm{L_i}}^{\mathrm{MM}\rightarrow\mathrm{QM/MM}}$, or individually for the simulations of the ligand bound to the host or free in solution. For the Bz, MeBz and Hx ligands, four or two independent results are presented, as has been explained before.

$\mathrm{L_i}$	$t_{\mathrm{eq}}(\Delta\Delta G)$	$t_{\mathrm{eq}}(\Delta G^{bound})$	$t_{\mathrm{eq}}(\Delta G^{free})$
Bz	2	3	4
	2	3	4
	3	3	4
	3	2	5
MeBz	2	8	4
	5	3	6
EtBz	1	4	4
pClBz	1	4	4
Hx	0	2	4
	0	2	6
	0	10	4
	0	2	5
MeHx	0	2	4
Pen	0	2	2
Hep	1	3	3

3.3 Number of independent simulations

To thoroughly converge $\Delta\Delta G_{\mathrm{L_i}}^{\mathrm{MM}\rightarrow\mathrm{QM/MM}}$, we have so far assumed that 100 snapshots are required. However, it is clear from the results in Figure 1 that the standard errors are very small ($\sim$0.1 kJ mol^{-1} for 50 ps simulation time), indicating that the number of snapshots may be reduced without compromising the accuracy. To test this, we performed bootstrap simulations with 5000 samples to estimate the standard error of the mean as a function of the number of included snapshots for three simulation times (10, 20 and 50 ps). The results are presented in Figure 4 for all nine ligands.

It can be seen that for all ligands except mClBz (which we already have discussed in detail), the standard error falls rapidly off for the full 50 ps simulations. Besides, mClBz, the Bz ligand shows the slowest convergence (Figure 4G), so we concentrate on this ligand. The precision in our previous study of $\Delta\Delta G_{\mathrm{L_i}}^{\mathrm{MM}\rightarrow\mathrm{QM/MM}}$ in this system was 0.4 kJ mol^{-1} for most ligands using four Λ values. This value is marked by a dashed horizontal line in Figure 4.

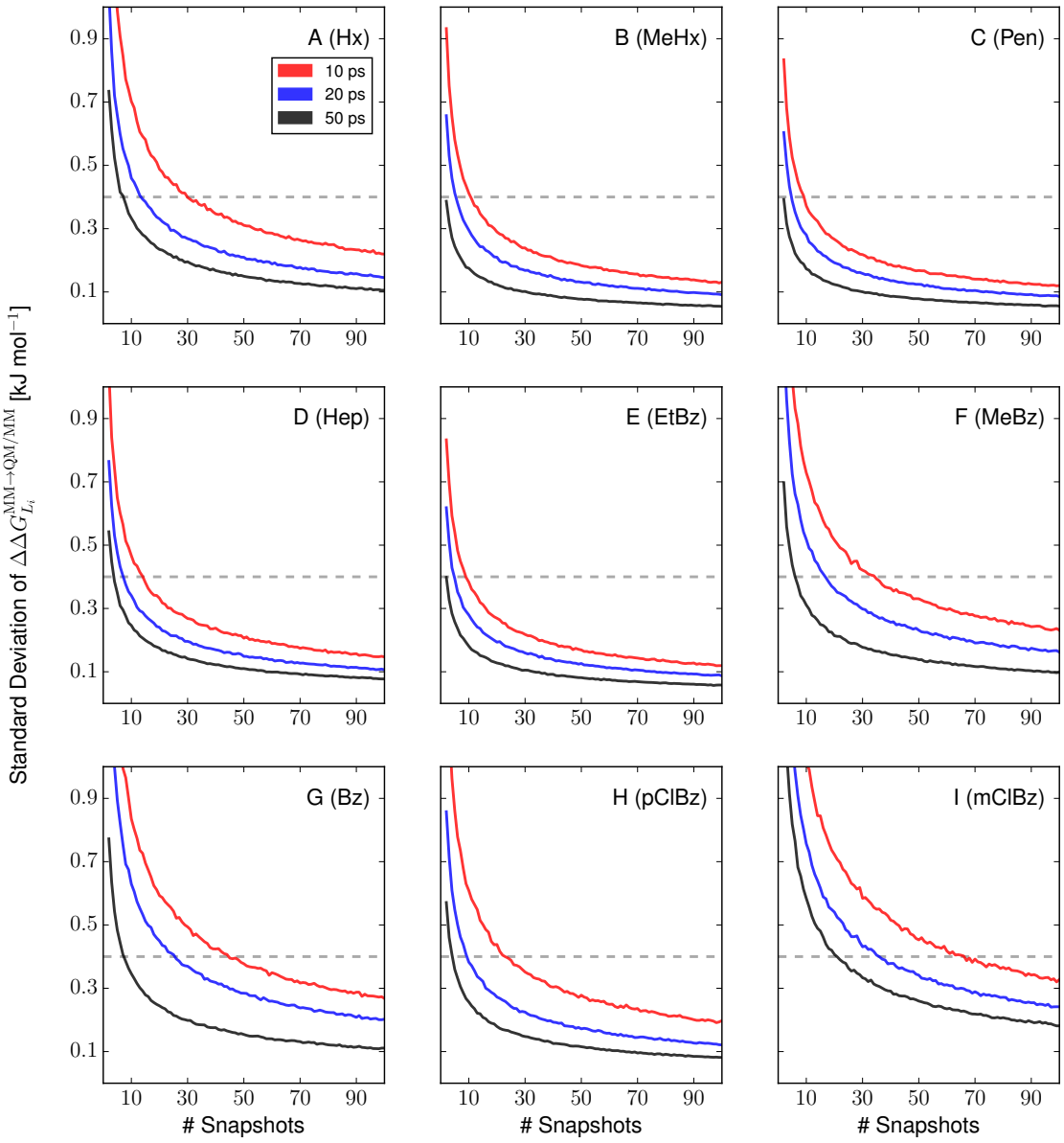

Figure 4: Simulated standard error of the free energy change $\Delta\Delta G_{\mathrm{L_i}}^{\mathrm{MM\rightarrow QM/MM}}$ using bootstrapping.

For such a precision the Bz ligand requires 45, 25 and 8 snapshots using simulations of lengths 10 ps, 20 ps and 50 ps, respectively. Based on these results, we suggest as a compromise between accuracy and computational effort to use 20 simulations of 20 ps of simulation time in each Λ-window (**OPT0**). In Table 2, $\Delta\Delta G_{\mathrm{L_i}}^{\mathrm{MM\rightarrow QM/MM}}$ results for **OPT0** are presented (employing every fifth snapshot out of the original 100) for each ligand. In general, the results

Table 2: Computed $\Delta\Delta G_{\mathrm{L_i}}^{\mathrm{MM}\rightarrow\mathrm{QM/MM}}$ values for all nine ligands using various strategies (described in the text). Energies are in kJ mol^{-1}, equilibration times in ps. As usual, two or four independent results are given for Bz, MeBz and Hx.

L_i	**OPT0**	**OPT1**	n_s	**OPT2**	n_s	t_{eq}	$\Lambda = 4^a$	$\Lambda = 9^a$
Bz	-0.1 ± 0.5	-0.6 ± 0.3	43	-0.4 ± 0.3	43	1	-0.3 ± 0.4	-1.0 ± 0.5
	-1.1 ± 0.4	-1.7 ± 0.3	32	-1.5 ± 0.3	32	1	-0.3 ± 0.4	-0.9 ± 0.5
	-1.2 ± 0.4	-1.4 ± 0.3	33	-1.4 ± 0.3	33	1	-0.8 ± 0.4	-1.0 ± 0.5
	-1.7 ± 0.5	-1.4 ± 0.3	43	-1.3 ± 0.3	43	1	-0.7 ± 0.4	-0.8 ± 0.5
MeBz	-0.4 ± 0.4	-0.3 ± 0.3	18	-0.2 ± 0.3	18	3	-0.6 ± 0.4	-1.3 ± 0.5
	-1.0 ± 0.4	-0.9 ± 0.3	31	-0.7 ± 0.3	31	1	-0.3 ± 0.4	-0.8 ± 0.5
EtBz	2.6 ± 0.3	2.2 ± 0.3	24	2.3 ± 0.3	30	2	1.9 ± 0.4	2.1 ± 0.5
pClBz	-5.4 ± 0.3	-5.8 ± 0.3	18	-5.5 ± 0.3	19	2	-5.0 ± 0.3	-5.5 ± 0.5
Hx	3.1 ± 0.2	2.7 ± 0.3	7	2.7 ± 0.2	8	3	2.9 ± 0.3	2.9 ± 0.4
	2.5 ± 0.2	1.8 ± 0.3	5	1.8 ± 0.2	5	2	2.1 ± 0.4	2.7 ± 0.4
	3.0 ± 0.2	3.3 ± 0.3	17	3.2 ± 0.3	17	1	3.3 ± 0.3	2.7 ± 0.4
	3.0 ± 0.2	3.3 ± 0.3	5	3.2 ± 0.3	5	1	3.6 ± 0.3	3.0 ± 0.4
MeHx	-0.6 ± 0.3	-1.0 ± 0.3	13	-1.1 ± 0.3	13	1	-0.6 ± 0.3	-0.6 ± 0.4
Pen	3.0 ± 0.2	2.8 ± 0.3	6	2.8 ± 0.3	6	0	2.9 ± 0.3	2.4 ± 0.5
Hep	2.2 ± 0.3	2.1 ± 0.3	13	2.1 ± 0.3	13	0	2.1 ± 0.4	0.9 ± 0.4

[a] previous results taken from Ref 14.

agree with reference results from our previous work[14] but obtained at almost a fourth of the computational cost (20 simulations of 20 ps correspond to a total simulation time of 400 ps, compared to 1.5 ns simulations in each Λ-window used previously; other parameters, such as the number of λ values, the time step, the number of ligands, legs and states, are the same). For example, the pClBz ligand is predicted to have a $\Delta\Delta G_{\mathrm{pClBz}}^{\mathrm{MM}\rightarrow\mathrm{QM/MM}}$ value of -5.4 ± 0.3 kJ mol^{-1} which is statistically equivalent to -5.0 ± 0.3 kJ mol^{-1} and -5.5 ± 0.5 kJ mol^{-1} obtained previously using four and nine Λ-values, respectively. The mean absolute deviation is 0.4 and 0.5 kJ mol^{-1} from the results with four and nine Λ values, respectively, and the maximum deviation is 1.0 and 1.3 kJ mol^{-1}, always within the 95% confidence intervals. Not unexpectedly, using a fixed number of snapshot gives rise to a varying precision with standard errors varying between 0.5 kJ mol^{-1} for Bz and 0.2 kJ mol^{-1} for most of the non-aromatic ligands, which is in agreement with the presented in Figure 4 above. We have again excluded the diverging mClBz ligand.

Alternatively, we may want to specify the desired precision of the results then perform

the number of simulations needed to reach such a precision (this is easily obtained by first performing a few simulations, then calculating the standard error and use the expected square-root dependence to estimate the number of simulations needed). On the other hand, such an approach (**OPT1**) gives rise to a varying computational cost for the various ligands. In Table 2 results for **OPT1** are presented with a precision of 0.3 kJ mol^{-1} (still with 20 ps simulation time) together with the required number of snapshots, n_{s}. The results are very similar to the **OPT0** results, showing differences of up to 0.7 kJ mol^{-1} (for one of the calculations with the Hx ligand), but in general less than 0.3 kJ mol^{-1} for the other ligands. As expected, n_{s} was less than 20 for the non-aromatic ligands ($n_{\mathrm{s}} = 5$–17). For the aromatic ligands, n_{s} is between 18 (MeBz and pClBz) and 43 (Bz). The mean absolute deviations from the $\Delta\Delta G_{\mathrm{L_i}}^{\mathrm{MM}\rightarrow\mathrm{QM/MM}}$ results obtained with four and nine Λ values are again 0.4 and 0.5 kJ mol^{-1}, respectively, with maximum deviations of 1.4 and 1.2 kJ mol^{-1}.

We also incorporated our equilibration approach discussed in Section 3.2. We use the procedure outlined for **OPT1** to initially obtain $\Delta\Delta G_{\mathrm{L_i}}^{\mathrm{MM}\rightarrow\mathrm{QM/MM}}$ with a precision of 0.3 kJ mol^{-1}. This was followed by the equilibration procedure, in which initial parts of the simulation were discarded based on the inequality in eq 6. If the standard error increased by discarding the equilibration data, n_{s} was increased by one and the equilibration procedure was repeated. Computed values of $\Delta\Delta G_{\mathrm{L_i}}^{\mathrm{MM}\rightarrow\mathrm{QM/MM}}$ together with the number of snapshots n_{s} and equilibration times t_{eq} are also presented in Table 2 with this approach (**OPT2**). We find that the aromatic ligands require at least some equilibration (Bz, MeBz and pClBz has $t_{\mathrm{eq}} = 1$–3 ps) which is consistent with the results in obtained in Table 1. The computed mean absolute deviation was found to be 0.4 and 0.5 kJ mol^{-1}, respectively. The corresponding maximum deviations were 1.2 and 1.2 kJ mol^{-1}, respectively, quite similar to the other two procedures. The computational load of the OPT1 and OPT2 methods is similar to that of OPT0 on average, giving a speedup of 3.6–4.1 compared to our previous simulations[14] (depending on how the average is calculated). However, for some calculations ligands, requiring only a few snapshots, the speedup is larger, up to a factor of 15 for two of

the Hx calculations.

Finally, we note that it is also possible to estimate the convergence of the results through overlap measures. This was done thoroughly in our previous studies of the same and other systems.[14,21,25] The conclusion was that the Π bias metric by Wu and Kofke[47] gave the most reliable results. Therefore, we have investigated the Π value for all individual simulations. The results, presented in Figure S16, shows that all simulations give $\Pi > 0$, indicating a proper overlap between the two energy distributions (MM and QM/MM).[47] In fact, only five simulations give $\Pi < 0.5$, which has been suggested as a heuristic safety margin.[47] In principle, simulations with $\Pi < 0.5$ could be discarded, elongated or re-run using five or more Λ-windows but this was not tested in this work.

4 Conclusions

We have presented a new efficient approach to compute free energy at the QM/MM level with the reference-potential method, which shows promising convergence properties. This new approach uses extensive conformational sampling at the MM level combined with multiple short QM/MM MD simulations to compute free energies at the QM/MM level. Such a combination provides a fast way to converge MM→QM/MM free energies and requires about four times shorter QM/MM MD simulations than in our previous investigation with standard QM/MM FEP calculations.[14] However, the computational load is still very significant, requiring 6.4 million QM evaluations per perturbation. To test our method, we studied the MM→QM/MM contribution to the binding free energies for nine cyclic carboxylate ligands bound to the octa-acid host from the SAMPL4 competition. We found that the method performs well for eight out of the nine ligands. For one ligand, the convergence is slower and the problem was traced to too large a difference in the MM and QM/MM potentials which consequently required the QM/MM MD simulations to overcome a slow conformational change.

We found that it was not necessary to use QM/MM minimizations before running the MD simulations. However, we find that the aromatic ligands gain somewhat from removing the first 1–5 ps of the simulations as equilibration. Overlap measures were computed for all ligands in the four Λ-windows and it was found that all of our results had appropriately overlapping energy distributions.

We finally note that with this approach, the efficiency is comparable to employing Jarzynski's equation for the non-equilibrium work, which has been employed in some studies.[48] In a future publication, we will compare the accuracy, precision and efficiency of these two approaches.

Acknowledgement

This work was supported by the Swedish Research Council (project 2014-5540) and the Knut and Alice Wallenberg Foundation (KAW 2013.022). C. S. thanks the Danish Council for Independent Research (the Sapere Aude program) for financial support (Grant no. DFF 4181-00370). The computations were performed on computer resources provided by the Swedish National Infrastructure for Computing (SNIC) at Lunarc at Lund University and HPC2N at Umeå University

Supporting Information Available

The supporting information contains additional calculations to support the conclusions in the manuscript. This includes: Verification of convergence dependending on the number of Λ-values, binding affinities for the ligands if minimization is used before the molecular dynamics simulation, a detailed discussion on the origin of the poor mClBz performance including structures to highlight the origin of the problem and additional figures related to convergence when using equilibration and overlap measures. This material is available free of charge via the Internet at `http://pubs.acs.org/`.

References

(1) Zwanzig, R. W. High-Temperature Equation of State by a Perturbation Method. I. Nonpolar Gases. *J. Chem. Phys.* **1954**, *22*, 1420–1426.

(2) Kirkwood, J. G. Statistical Mechanics of Fluid Mixtures. *J. Chem. Phys.* **1935**, *3*, 300–313.

(3) Bennett, C. H. Efficient estimation of free energy differences from Monte Carlo data. *J. Comput. Phys.* **1976**, *22*, 245–268.

(4) Shirts, M. R.; Pande, V. S. Comparison of efficiency and bias of free energies computed by exponential averaging, the Bennett acceptance ratio, and thermodynamic integration. *J. Chem. Phys.* **2005**, *122*, 144107.

(5) Gilson, M.; Given, J.; Bush, B.; McCammon, J. The statistical-thermodynamic basis for computation of binding affinities: a critical review. *Biophys. J.* **1997**, *72*, 1047–1069.

(6) Hansen, N.; van Gunsteren, W. F. Practical Aspects of Free-Energy Calculations: A Review. *J. Chem. Theory Comput.* **2014**, *10*, 2632–2647.

(7) Christ, C. D.; Mark, A. E.; van Gunsteren, W. F. Basic ingredients of free energy calculations: A review. *J. Comput. Chem.* **2009**, NA–NA.

(8) Ryde, U.; Söderhjelm, P. Ligand-Binding Affinity Estimates Supported by Quantum-Mechanical Methods. *Chem. Rev.* **2016**, *116*, 5520–5566.

(9) Senn, H. M.; Thiel, W. QM/MM Methods for Biomolecular Systems. *Angew. Chem. Int. Ed.* **2009**, *48*, 1198–1229.

(10) Ryde, U. In *Computational Approaches for Studying Enzyme Mechanism Part A*; Voth, G. A., Ed.; Methods in Enzymology; Elsevier, 2016; Vol. 577; Chapter 6, pp 119–158.

(11) Reddy, M. R.; Erion, M. D. Relative Binding Affinities of Fructose-1, 6-Bisphosphatase Inhibitors Calculated Using a Quantum Mechanics-Based Free Energy Perturbation Method. *J. Am. Chem. Soc.* **2007**, *129*, 9296–9297.

(12) Rathore, R. S.; Reddy, R. N.; Kondapi, A. K.; Reddanna, P.; Reddy, M. R. Use of quantum mechanics/molecular mechanics-based FEP method for calculating relative binding affinities of FBPase inhibitors for type-2 diabetes. *Theor. Chem. Acc.* **2012**, *131*.

(13) Świderek, K.; Martí, S.; Moliner, V. Theoretical studies of HIV-1 reverse transcriptase inhibition. *Phys. Chem. Chem. Phys.* **2012**, *14*, 12614.

(14) Olsson, M. A.; Ryde, U. Comparison of QM/MM Methods To Obtain Ligand-Binding Free Energies. *J. Chem. Theory Comput.* **2017**, *13*, 2245–2253.

(15) Luzhkov, V.; Warshel, A. Microscopic models for quantum mechanical calculations of chemical processes in solutions: LD/AMPAC and SCAAS/AMPAC calculations of solvation energies. *J. Comput. Chem.* **1992**, *13*, 199–213.

(16) Gao, J. Absolute free energy of solvation from Monte Carlo simulations using combined quantum and molecular mechanical potentials. *J. Phys. Chem.* **1992**, *96*, 537–540.

(17) Gao, J.; Xia, X. A priori evaluation of aqueous polarization effects through Monte Carlo QM-MM simulations. *Science* **1992**, *258*, 631–635.

(18) Rod, T. H.; Ryde, U. Quantum Mechanical Free Energy Barrier for an Enzymatic Reaction. *Phys. Rev. Lett.* **2005**, *94*.

(19) Rod, T. H.; Ryde, U. Accurate QM/MM Free Energy Calculations of Enzyme Reactions: Methylation by CatecholO-Methyltransferase. *J. Chem. Theory Comput.* **2005**, *1*, 1240–1251.

(20) Duarte, F.; Amrein, B. A.; Blaha-Nelson, D.; Kamerlin, S. C. Recent advances in QM/MM free energy calculations using reference potentials. *Biochim. Biophys. Acta, Gen. Subj.* **2015**, *1850*, 954–965.

(21) Olsson, M. A.; Söderhjelm, P.; Ryde, U. Converging Ligand-Binding Free Energies Obtained with Free-Energy Perturbations at the Quantum Mechanical Level. *J. Comput. Chem.* **2016**, *37*, 1589–1600.

(22) Knig, G.; Boresch, S. Non-Boltzmann sampling and Bennett's acceptance ratio method: How to profit from bending the rules. *J. Comput. Chem.* **2011**, *32*, 1082–1090.

(23) Jia, X.; Wang, M.; Shao, Y.; König, G.; Brooks, B. R.; Zhang, J. Z. H.; Mei, Y. Calculations of Solvation Free Energy through Energy Reweighting from Molecular Mechanics to Quantum Mechanics. *J. Chem. Theory Comput.* **2016**, *12*, 499–511.

(24) Beierlein, F. R.; Michel, J.; Essex, J. W. A Simple QM/MM Approach for Capturing Polarization Effects in Protein-Ligand Binding Free Energy Calculations. *J. Phys. Chem. B.* **2011**, *115*, 4911–4926.

(25) Mikulskis, P.; Cioloboc, D.; Andrejić, M.; Khare, S.; Brorsson, J.; Genheden, S.; Mata, R. A.; Söderhjelm, P.; Ryde, U. Free-Energy Perturbation and Quantum Mechanical Study of SAMPL4 Octa-Acid Host–Guest Binding Energies. *J. Comput. Aided Mol. Des.* **2014**, *28*, 375–400.

(26) Genheden, S.; Ryde, U.; Söderhjelm, P. Binding affinities by alchemical perturbation using QM/MM with a large QM system and polarizable MM model. *J. Comput. Chem.* **2015**, *36*, 2114–2124.

(27) Sampson, C.; Fox, T.; Tautermann, C. S.; Woods, C.; Skylaris, C.-K. A "Stepping Stone" Approach for Obtaining Quantum Free Energies of Hydration. *J. Phys. Chem. B.* **2015**, *119*, 7030–7040.

(28) Hummer, G.; Szabo, A. Calculation of free-energy differences from computer simulations of initial and final states. *J. Chem. Phys.* **1996**, *105*, 2004–2010.

(29) Kästner, J.; Senn, H. M.; Thiel, S.; Otte, N.; Thiel, W. QM/MM Free-Energy Perturbation Compared to Thermodynamic Integration and Umbrella Sampling: Application to an Enzymatic Reaction. *J. Chem. Theory Comput.* **2006**, *2*, 452–461.

(30) Woods, C. J.; Manby, F. R.; Mulholland, A. J. An efficient method for the calculation of quantum mechanics/molecular mechanics free energies. *J. Chem. Phys.* **2008**, *128*, 014109.

(31) Woods, C. J.; Shaw, K. E.; Mulholland, A. J. Combined Quantum Mechanics/Molecular Mechanics (QM/MM) Simulations for Protein–Ligand Complexes: Free Energies of Binding of Water Molecules in Influenza Neuraminidase. *J. Phys. Chem. B.* **2015**, *119*, 997–1001.

(32) Plotnikov, N. V.; Kamerlin, S. C. L.; Warshel, A. Paradynamics: An Effective and Reliable Model for Ab Initio QM/MM Free-Energy Calculations and Related Tasks. *J. Phys. Chem. B.* **2011**, *115*, 7950–7962.

(33) Plotnikov, N. V.; Warshel, A. Exploring, Refining, and Validating the Paradynamics QM/MM Sampling. *J. Phys. Chem. B.* **2012**, *116*, 10342–10356.

(34) Lameira, J.; Kupchencko, I.; Warshel, A. Enhancing Paradynamics for QM/MM Sampling of Enzymatic Reactions. *J. Phys. Chem. B.* **2016**, *120*, 2155–2164.

(35) Gibb, C. L. D.; Gibb, B. C. Binding of cyclic carboxylates to octa-acid deep-cavity cavitand. *J. Comput. Aided Mol. Des.* **2013**, *28*, 319–325.

(36) Muddana, H. S.; Fenley, A. T.; Mobley, D. L.; Gilson, M. K. The SAMPL4 host–guest blind prediction challenge: an overview. *J. Comput. Aided Mol. Des.* **2014**, *28*, 305–317.

(37) Wang, J.; Wolf, R. M.; Caldwell, J. W.; Kollman, P. A.; Case, D. A. Development and Testing of a General Amber Force Field. *J. Comput. Chem.* **2004**, *25*, 1157–1174.

(38) Bayly, C. I.; Cieplak, P.; Cornell, W.; Kollman, P. A. A well-behaved electrostatic potential based method using charge restraints for deriving atomic charges: the RESP model. *J. Phys. Chem.* **1993**, *97*, 10269–10280.

(39) Case, D. A.; Betz, R.; Cerutti, D. S.; Cheatham, T. E.; III,; Darden, T. A.; Duke, R. E.; Giese, T. J.; Gohlke, H.; Goetz, A. W.; Homeyer, N.; Izadi, S.; Janowski, P.; Kaus, J.; Kovalenko, A.; Lee, T. S.; LeGrand, S.; Li, P.; Lin, C.; Luchko, T.; Luo, R.; Madej, B.; Mermelstein, D.; Merz, K. M.; Monard, G.; Nguyen, H.; Nguyen, H. T.; Omelyan, I.; Onufriev, A.; Roe, D.; Roitberg, A.; Sagui, C.; Simmerling, C. L.; Botello-Smith, W. M.; Swails, J.; Walker, R. C.; Wang, J.; Wolf, R. M.; Wu, X.; Xiao, L.; Kollman, P. A. AMBER 2014. *University of California, San Francisco.* **2014**,

(40) Walker, R. C.; Crowley, M. F.; Case, D. A. The implementation of a fast and accurate QM/MM potential method in Amber. *J. Comput. Chem.* **2008**, *29*, 1019–1031.

(41) Korth, M. Third-Generation Hydrogen-Bonding Corrections for Semiempirical QM Methods and Force Fields. *J. Chem. Theory Comput.* **2010**, *6*, 3808–3816.

(42) Wu, X.; Brooks, B. R. Self-guided Langevin dynamics simulation method. *Chem. Phys. Lett.* **2003**, *381*, 512–518.

(43) Berendsen, H. J. C.; Postma, J. P. M.; van Gunsteren, W. F.; DiNola, A.; Haak, J. R. Molecular dynamics with coupling to an external bath. *J. Chem. Phys.* **1984**, *81*, 3684–3690.

(44) Darden, T.; York, D.; Pedersen, L. Particle mesh Ewald: An N·log(N) method for Ewald sums in large systems. *J. Chem. Phys.* **1993**, *98*, 10089–10092.

(45) Shirts, M. R.; Chodera, J. D. Statistically optimal analysis of samples from multiple equilibrium states. *J. Chem. Phys.* **2008**, *129*, 124105.

(46) Nicholls, A. Confidence limits, error bars and method comparison in molecular modeling. Part 2: comparing methods. *J. Comput. Aided Mol. Des.* **2016**, *30*, 103–126.

(47) Wu, D.; Kofke, D. A. Phase-space overlap measures. I. Fail-safe bias detection in free energies calculated by molecular simulation. *J. Chem. Phys.* **2005**, *123*, 054103.

(48) Hudson, P. S.; Woodcock, H. L.; Boresch, S. Use of Nonequilibrium Work Methods to Compute Free Energy Differences Between Molecular Mechanical and Quantum Mechanical Representations of Molecular Systems. *J. Phys. Chem. Lett.* **2015**, *6*, 4850–4856.

Graphical TOC Entry